

Biomimetic calcium phosphate coating on electrospun poly(ϵ -caprolactone) scaffolds for bone tissue engineering

F. Yang*, J.G.C. Wolke, J.A. Jansen

*Department of Periodontology and Biomaterials, Radboud University Nijmegen Medical Center,
P.O. Box 9101, 6500 HB, Nijmegen, The Netherlands*

Received 1 May 2007; received in revised form 18 July 2007; accepted 19 July 2007

Abstract

The aim of this study is to develop a facile and efficient process to provide electrospun poly(ϵ -caprolactone) (PCL) scaffold with a bone-like calcium phosphate (CaP) coating while maintaining its fibrous and porous structure. Firstly, PCL scaffolds with uniform fibrous structure were fabricated by electrospinning. Before CaP coating, a plasma surface treatment was applied to clean and activate the PCL surface for calcium and phosphate ion grafting. Then, the treated PCL scaffolds were immersed in 10 \times simulated body fluid (SBF10) for varying time periods. PCL fibers were found to be mineralized after immersion in SBF10 for 2 h (SBF10_2h). After 6 h, the PCL scaffolds (SBF10_6h) were fully covered with CaP coating and the porous structure was lost. The coating of SBF10_2h was determined to consist of a mixture of nano-apatite and dicalcium phosphate dihydrate (DCPD). By continuous immersion in classical SBF for 7 days, the coating transformed into pure calcium deficient type B carbonate apatite with nano-crystallinity, which was similar to biological apatite. The deposited calcium phosphate coatings improved the wettability of the electrospun PCL scaffold. As the mineralized electrospun scaffold has a similar structure as the natural bone, it is expected to be a potential cell carrier in bone tissue engineering.

© 2007 Elsevier B.V. All rights reserved.

Keywords: Electrospinning; Biomimetic coating; Plasma treatment; Apatite; Brushite; Polycaprolactone; Biodegradable polymer

1. Introduction

It is estimated that more than 500,000 bone-grafting procedures are performed annually in the United States [1]. The number easily doubles on a global basis and will increase in the next year due to the ageing of the population. The increasing number of bone-grafting procedures has created a shortage in the availability of musculoskeletal donor tissue, as is traditionally used in reconstructive surgery. This has stimulated corporate interest in developing and supplying a rapidly expanding number of bone substitutes [1]. It is in this background that an emerging field of science called tissue engineering has been gaining interest in the last 10 years.

Engineering bone for reconstructive surgery requires three basis elements: an appropriate cell source, optimal signals for cell functioning and a (biodegradable) scaffold to serve as a temporary extracellular matrix (ECM). The requirements for the

design and production of an ideal scaffold are very complex and not yet fully understood. It is accepted that fibers are particularly suitable for use as scaffolding components compared to other structures, e.g. particles, due to their continuous structure. The advantages of a scaffold composed of ultrafine, continuous fibers are high porosity, variable pore-size distribution, high surface-to-volume ratio, and most importantly, morphological similarity to natural ECM [2].

To fabricate fibrous scaffolds mimicking the natural ECM structure, electrospinning, also called electrical spinning, has attracted tremendous interest in the research community simply because it provides a facile and effective means to produce ultrafine fibers with diameters ranging from microns down to a few nanometers. The process involves the use of an electric field to convert the polymer solution into continuous polymer fibers. The resulting fibers are in the form of a non-woven structure. So far, a lot of research efforts have been made to study the efficacy of electrospun scaffolds for tissue engineering applications [3,4], including bone tissue engineering [2,5,6].

Besides the architecture of the scaffolds, the surface chemistry is also crucial as it provides the direct contact with the

* Corresponding author. Tel.: +31 24 361 4086; fax: +31 24 361 4657.
E-mail address: f.yang@dent.umcn.nl (F. Yang).

surrounding cells and tissues. Although polymeric materials alone have shown some positive results for bone regeneration [5,7], efforts have been made to enhance and stimulate their bone response by coating them with a layer of bone-like apatite or calcium phosphate (CaP) ceramic [8–10]. Therefore, it is expected that such a coating may also improve the bone behavior of electrospun scaffolds. Compared with coating polymeric films or other porous structures, the coating of electrospun fibers is more challenging. In addition to making a compatible surface for apatite crystals to grow, it also requires getting a very uniform coating around the ultrafine fibers, including those in the center of the scaffold and controlling that the coating does not block the pores in the scaffold. Unfortunately, to our knowledge, only a limited amount of research has been done to study the coating of electrospun scaffolds [11,12]. Ito et al. [11] reported a biomimetic process to coat electrospun poly(3-hydroxybutyrate-co-3-hydroxyvalerate) (PHBV) with hydroxyapatite. However, the electrospun scaffold was fully covered by the coating and had no sign of porous structure. Chen et al. [12] successfully coated electrospun poly(lactic acid) (PLLA) with a thin layer of flake-like carbonated apatite, but the process lasted for up to 28 days. Therefore, the aim of this study was to coat electrospun scaffold fast and efficiently with the bone-like apatite, while maintaining its fibrous and porous structure.

2. Materials and methods

2.1. Fabrication of poly(ϵ -caprolactone) (PCL) scaffold

In this study, the electrospun poly(ϵ -caprolactone) (PCL) scaffold was prepared from PCL/2,2,2-trifluoroethanol (TFE) solution. PCL with Mn of 80,000 was purchased from Sigma–Aldrich and TFE was bought from Acros Organics. In order to obtain a fine fibrous morphology, the concentration of PCL solution was varied in the range from 8 to 12% (w/v). A commercially available electrospinning set-up (Advanced Surface Technology, Bleiswijk, The Netherlands) was used for the scaffold fabrication, similar as described previously [13]. From each concentration of PCL solution, 10 ml was fed into a glass syringe, which was controlled by a syringe pump (KD Scientific Inc., USA) at a feeding rate of 1.5 ml/h. A Teflon tube was used to connect the syringe and a blunt-end nozzle with an inner diameter of 0.5 mm, which was set up vertically. The distance between the nozzle and collector was adjusted to 15 cm. A high voltage of 12 kV was applied to generate the polymer jet. The resulting PCL fibers were collected on a piece of alumina foil, left in a fume hood overnight to eliminate the solvent residue and kept in a desiccator for further characterization and treatment.

In addition to electrospun scaffolds, PCL films were also made from 10% (w/v) PCL/chloroform solution by solvent casting. In brief, 10 ml PCL solution was cast onto a 15-cm diameter glass Petri dish and then left in a fume hood. After evaporation of the solvent, a piece of PCL film was removed from the Petri dish and used in some of the characterization assays.

Table 1

Solution preparation recipe for 1 l of classical simulated body fluid (SBF) and 10× concentrated SBF (SBF10)

Reagent	Order	Amount (g)	
		SBF ^a	SBF10 ^b
NaCl	1	7.995	58.430
KCl	2	0.224	0.373
CaCl ₂ ·2H ₂ O	3	0.368	3.675
MgCl ₂ ·6H ₂ O	4	0.305	1.016
Na ₂ HPO ₄	5	–	1.420
K ₂ HPO ₄	6	0.174	–
NaHCO ₃	7	0.349	0.840
Na ₂ SO ₄ ·10H ₂ O	8	0.161	–

^a SBF was buffered with tris(hydroxymethyl) aminomethane (50 mM) and set at pH 7.4 with 1.0 M hydrochloric acid.

^b NaHCO₃ was added just prior to coating under stirring at 500 rpm.

2.2. Biomimetic coating solutions

The classical SBF and 10× concentrated SBF (SBF10) solutions were prepared by changing salt concentrations as summarized in Table 1. The preparation of SBF followed Kokubo's method [14] and the one for SBF10 was adopted from Tas and Bhaduri [15]. For all solutions, reagent grade chemicals and deionized water (Millipore, USA) were used. The final solutions were filtered to eliminate impurities. When SBF was prepared, the solution was buffered with tris(hydroxymethyl) aminomethane (50 mM) and finally set at pH 7.4 by using 1.0 M hydrochloric acid. In order to make the concentrated SBF10, a stock solution containing NaCl, KCl, CaCl₂·2H₂O, MgCl₂·6H₂O and Na₂HPO₄ was prepared in advance. This stock solution can be kept at 4 °C for several weeks without precipitation. NaHCO₃ was added just prior to the coating procedure under a stirring speed of 500 rpm. The calculated ion concentrations of SBF solutions in comparison with those in human blood plasma (HBP) are listed in Table 2.

2.3. Coating process

Samples with the dimension of 1 cm × 5 cm were cut from electrospun PCL sheets and PCL films. All the samples were argon plasma treated using a radio frequency glow discharge plasma cleaner (PDC-001, Harrick Scientific Corp., USA). Plasma discharge was applied to the samples for 10 min with the radio frequency power set at 30 W under vacuum condition.

After plasma treatment, the scaffolds were immersed into SBF10 in a tightly capped plastic tube and kept at room temperature for 2–6 h during coating. The SBF 10 solution

Table 2

Inorganic concentration (mM) of human blood plasma (HBP), SBF and SBF10

	Ca ²⁺	HPO ₄ ²⁻	Na ⁺	K ⁺	Mg ²⁺	Cl ⁻	HCO ₃ ⁻	SO ₄ ²⁻
HBP	2.5	1.0	142.0	5.0	1.5	103.0	27.0	0.5
SBF	2.5	1.0	142.0	5.0	1.5	147.8	4.2	0.5
SBF10	25.0	10.0	1030.0	5.0	5.0	1065.0	10.0	0

was changed after every 2 h. Some of the samples were continuously coated in SBF solution at 37 °C for another 7 days and the coating solution was refreshed every 2 days. When the coating process was finished, the samples were collected, cleaned with deionized water and freeze dried overnight.

2.4. Characterization of the electrospun scaffolds and the coatings

Non-coated and coated electrospun PCL scaffolds as well as films were characterized using the following techniques:

- Scanning electronic microscopy (SEM): the morphology of coated PCL scaffolds was investigated by using SEM (Jeol SEM6310, Japan) after gold sputtering. The fiber diameter was measured from the SEM micrographs taken at random locations.
- The porosity of the electrospun scaffolds was evaluated by using a gravimetric measurement [16]. In brief, the electrospun meshes were punched into 15-mm discs. After measuring the thickness, the volume of the scaffold could be determined. The mass of the scaffold was also measured for determination of the apparent density of the scaffold (ρ_{ap}). The porosity was then calculated according to the following equation:

$$\text{porosity} = \left(1 - \frac{\rho_{ap}}{\rho_m}\right) \times 100\% \quad (1)$$

where ρ_m is the density of the scaffold material, PCL ($\rho = 1.145 \text{ g/cm}^3$, Sigma–Aldrich MSDS database).

- X-ray diffraction (XRD): in order to determine the crystallographic structure of the coatings, a sufficient amount of coatings was scratched from the PCL films and was verified using a Philips θ – 2θ diffractometer with Cu K α -radiation (PW3710, 40 kV, 40 mA). The scanning range was from 10 to 40° with a step size of 0.02°. The crystal size of the apatite coating was estimated from Scherrer formula:

$$L = \frac{K\lambda}{(\beta_m - \beta) \cos \theta} \quad (2)$$

where λ is the X-ray wavelength, θ the diffraction angle, β_m the observed width of half height of the diffraction profile resulting from small crystallite size, β the instrument broadening (broadening measured with standard reference material lanthanum hexaboride (LaB₆, NIST 660a)) and K is shape constant equal to 0.9 in this study. (002) line of the apatite crystal was used for the calculation.

- Fourier-transform infrared spectrometry (FTIR): the same samples used in XRD study were also tested by a FTIR spectrometer (Spectrum One, Perkin-Elmer) in order to identify the chemical structure. Transmission infrared spectra were obtained from 4000 cm to 450 cm⁻¹ on pellets prepared by mixing 2 mg coating in 300 mg IR-grade KBr powder.
- Energy dispersive spectroscopy (EDS): to determine the composition of the coated CaP, EDS was performed using an

energy dispersive X-ray microanalyzer (Voyager, Noran) that is connected to the SEM. During collection of the spectra, the accelerating voltage was set to 10 kV.

- Microcomputer tomography (micro-CT): to examine the distribution of the mineral content in coated electrospun scaffolds, the samples were scanned using micro-CT equipment (Skyscan 1072, Skyscan, Aartselaar, Belgium) at a resolution of 2.36 μm per pixel.
- Water wettability test: a drop of 10 μl deionized water was applied on the surface of different scaffolds and films. The drops were photographed immediately and the contact angle (θ) was calculated from the height (h) and breadth (b) of the drop [17] according to

$$\theta = 2 \arctan \frac{2h}{b} \quad (3)$$

In this way, the wettability of each scaffold was measured in triplicate.

- Water capillary reaction study: electrospun scaffolds were tested using the method reported before [18]. In brief, one end of an electrospun sample was vertically dipped into a Petri dish filled with deionized water and the length of the scaffold underneath the water was 0.5 cm. After 30 s, the sample was taken out from the water and the upcoming water front line was recorded by a digital camera.

3. Results and discussion

3.1. Morphology of electrospun PCL fibers

As shown by previous studies, the morphology of polymer electrospun fibers was influenced by various polymer solution properties and processing parameters [3]. Among all the variables, solution viscosity as controlled by changing the polymer concentration has been found to be one of the major factors, which affect the fiber size and morphology. In this study, we fixed all processing parameters except for the PCL concentration. The SEM photographs (Fig. 1) depict the morphological differences among the fibers electrospun from 8 to 12% PCL solutions. The fiber diameters were measured from the SEM photographs and their distribution is shown in Fig. 2. The results indicated that all the electrospun scaffolds presented a three-dimensional porous fibrous mesh appearance consisting of random orientated PCL fibers. When the polymer concentration was increased, the mat morphology changed gradually from a bead-fiber structure to a spindle-fiber one, and finally in a uniform fiber structure. At the same time, the average fiber diameter increased from 100 nm to 1.5 μm . Those results are consistent with previous studies [3]. As it is supposed that the bead-fiber structure weakens the scaffold mechanical properties, the scaffolds fabricated from 12% PCL solution were used in the subsequent studies.

We further calculated the porosity of electrospun scaffolds made from 12% PCL solution, which was found to be $75.1 \pm 2.0\%$ ($n = 10$) indicating that the scaffold was highly porous. The estimated pore size was around 10 μm .

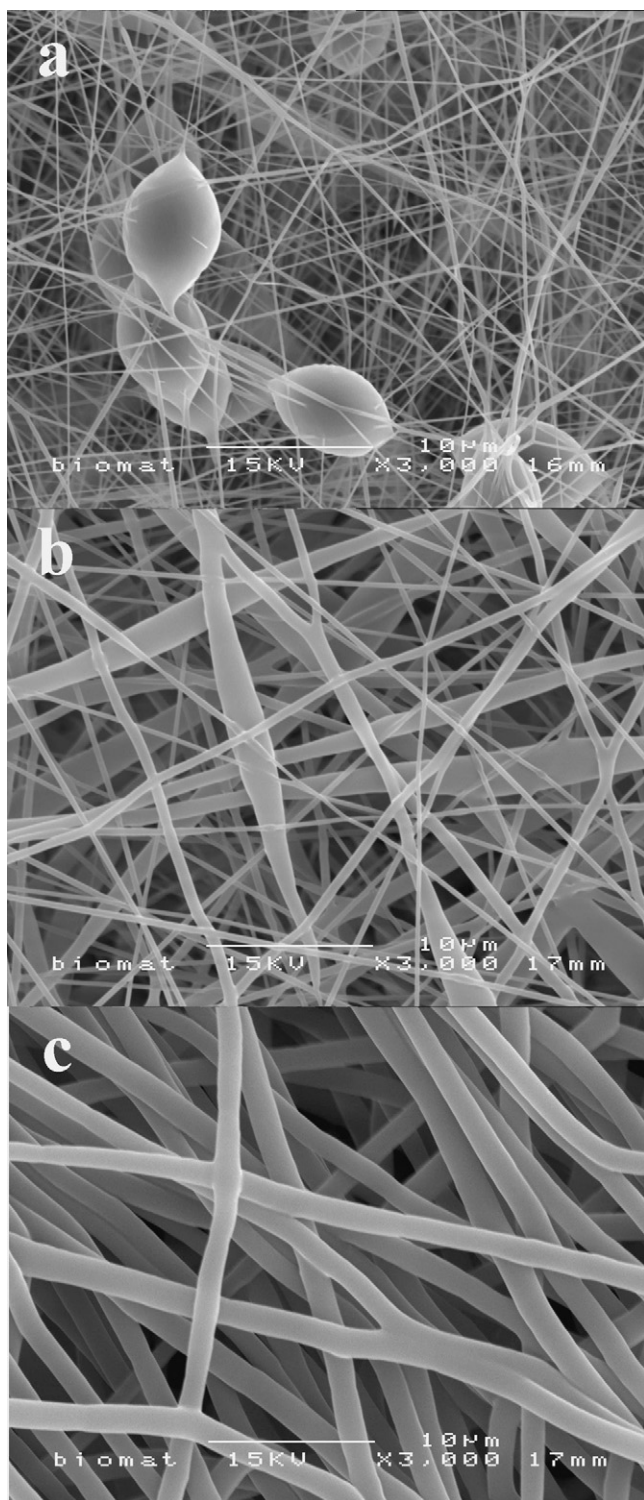


Fig. 1. SEM photographs of electrospun PCL fibers made from PCL/TFE solutions: (a) 8%, (b) 10% and (c) 12%.

3.2. Biomimetic coating

An appropriate polymer surface is crucial for CaP grafting or coating. However, PCL is inert when compared with other biopolymers, such as PLLA and PHBV, which results in heterogeneous mineral growth through carboxylic acid and hydroxyl

groups on the surface [11,12]. Therefore, it is necessary to modify the surface of PCL scaffolds in order to deposit a CaP coating. Recently, several methods have been used for the surface modification, such as NaOH [19] and plasma [20] treatment. As NaOH is toxic and the treatment period is as long as 48 h, plasma treatment is considered to be superior. A plasma is a partially ionized gas containing ions, electrons, atoms and neutral species, which react with the polymer surface (10–1000 Å of the substrate) without damaging the bulk properties. By plasma treatment, the weak chemical bondings of PCL are replaced by highly reactive carbonyl (–CO–), carboxyl (–COOH) and hydroxyl (–OH) groups [20]. The surface becomes super-active after treatment compared with an untreated polymer surface. The consequences are a decrease of the surface water contact angle and an increase in bonding sites for calcium and phosphate ions. When the scaffold is immersed in SBF solutions ($\text{pH} \leq 7.4$), the active carboxyl groups become carboxyl anions (–COO[–]). These negatively charged –COO[–] groups are ready to chelate the calcium and then phosphate ions in the solution. The bindings of these soluble ionic precursors stimulate surface nucleation [9].

SBF solutions are known to induce bone-like CaP formation on metals, ceramics and polymers after proper surface treatment. Although the classical SBF mimics the ion concentration, pH and the temperature of human blood plasma (HBF) [14], it

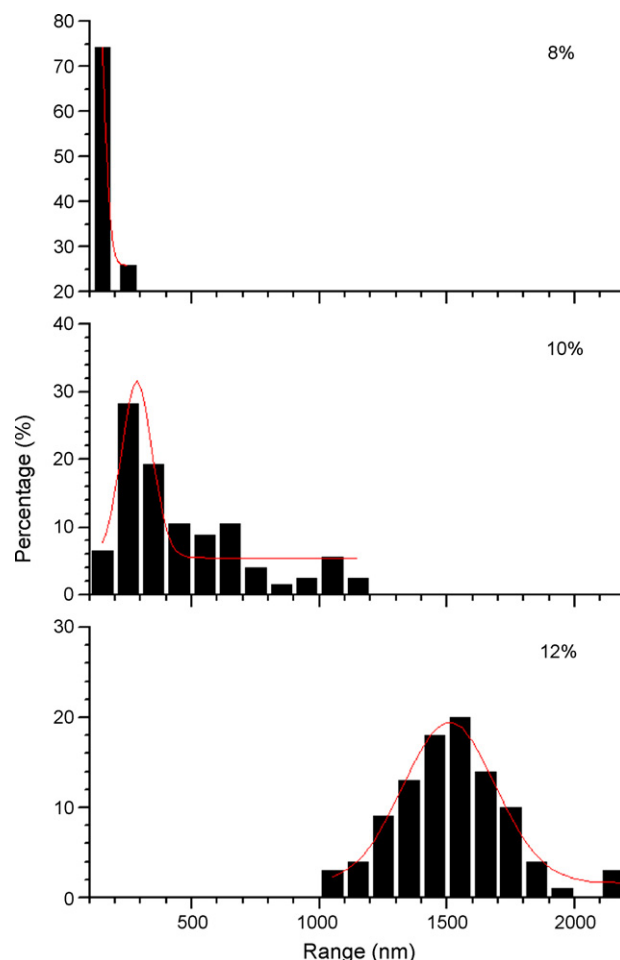


Fig. 2. The diameter distribution of the electrospun PCL fibers.

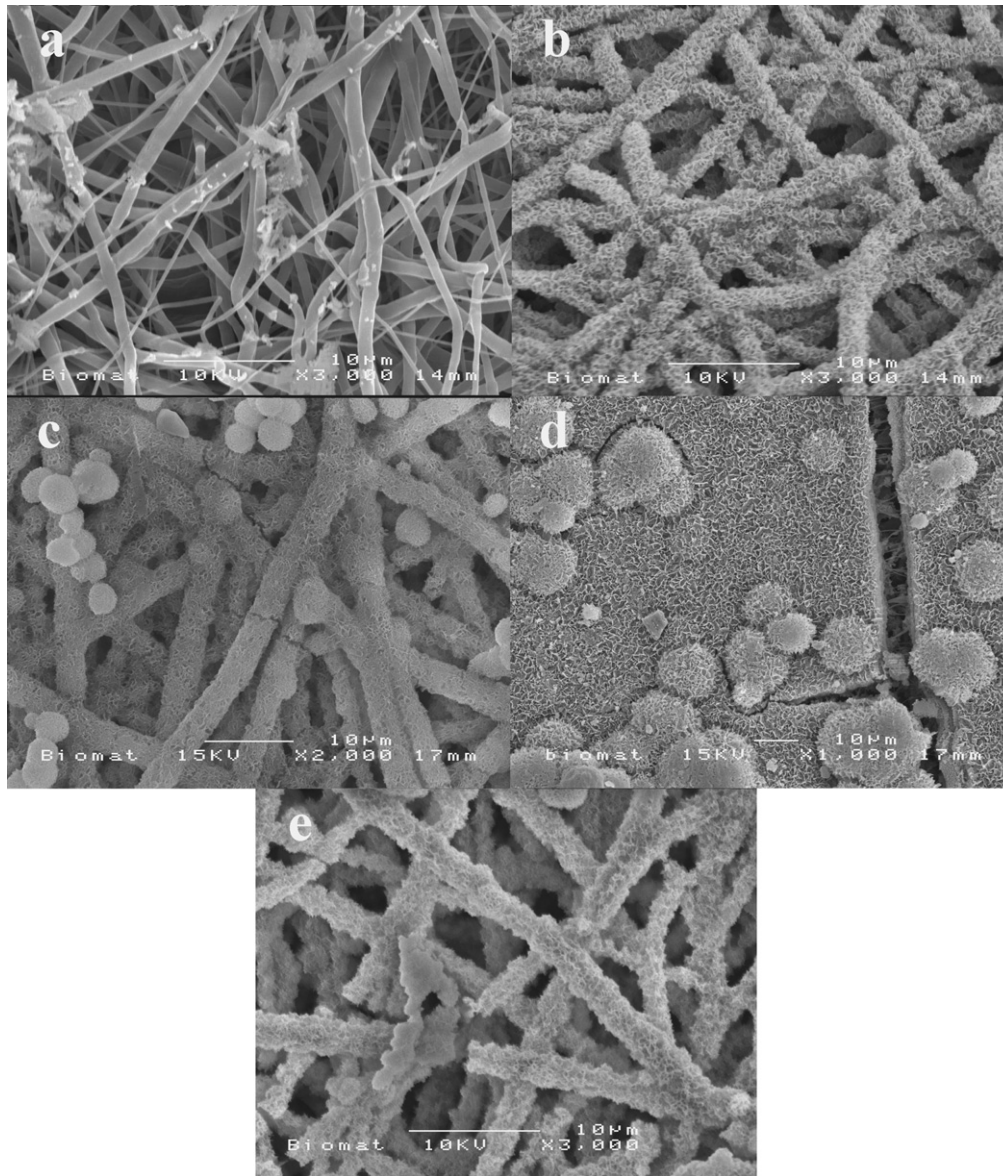


Fig. 3. SEM micrographs showing the surface of the electrospun PCL scaffolds after coating: (a) SBF10_1h, (b) SBF10_2h, (c) SBF10_3h, (d) SBF10_6h and (e) +SBF_7d.

is only slightly supersaturated with respect to precipitation of stoichiometric hydroxyapatite. Therefore, nucleation and precipitation of CaPs is rather slow, normally up to a few weeks. To accelerate the process, higher concentrated SBFs are used [15,21]. In this study, a 10× SBF solution was used for apatite coating.

Fig. 3 illustrates SEM photographs of coated PCL electrospun scaffolds after different coating periods. The changes of the fiber diameter and scaffold weight are listed in Table 3. For convenience, the samples coated in SBF10 for 1 h are termed as SBF10_1h, those coated for 2 h termed as SBF10_2h, and so on. After 1 h of incubation, the PCL fibers were almost intact except some tiny particles scattered on the fiber surface. Without any change in the fiber diameter, the scaffold gained 2.3% in weight. The results indicated that CaP just initiated to nucleate on the polymer surface. However, after 2 h of incubation, the

PCL fibers were fully surrounded with nano-textured flake-like CaP coatings, suggesting a homogenous nucleation and fast precipitation of the CaP. At the same time, the scaffold maintained its porous and fibrous structure and the average diameter of the fibers increased from 1.5 to 2.2 μm along with 8.3% increase in

Table 3

The average fiber diameter and weight change of the electrospun scaffolds after coating

Sample	Average fiber diameter (μm)	Weight change (%)
SBF10_1h	1.5 ± 0.2	2.3 ± 0.3
SBF10_2h	2.2 ± 0.5	8.3 ± 1.0
SBF10_3h	3.2 ± 0.6	13.5 ± 0.6
SBF10_6h	–	25.6 ± 1.5
+SBF_7d	2.3 ± 0.6	21.8 ± 1.9

weight. The increase in fiber diameter resulted in a decrease of the scaffold's pore size, which became less than $10\ \mu\text{m}$. When the scaffolds were kept in the coating solution up to 3 h, the fiber diameter continuously increased to $3.2\ \mu\text{m}$ and the weight rose to 13.5%. Besides, some CaP globules started to appear on the scaffold surface. After 6 h of incubation, the surface of the scaffold was fully covered with CaP coating and the fibrous structure was no longer visible. Based on these results, SBF10_2h appeared to be the most suitable material for tissue engineering application and was used for further studies since it showed uniform coatings of the fibers while maintaining the fibrous porous structure.

One of the advantages of electrospun scaffolds for tissue engineering application is their porous structure. Although the pore size of the electrospun PCL mats is around $10\ \mu\text{m}$, which is smaller than the cells, some evidence showed that cells could penetrate into the pores. Zhang et al. [2] found that the bone marrow stromal cells could infiltrate up to 48 and $114\ \mu\text{m}$ in the electrospun PCL and PCL/gelatin scaffold with the pore size of a few microns, respectively. Shin et al. [5] reported that the mesenchymal stem cells migrated into the whole electrospun PCL scaffold ($\sim 1\ \text{mm}$ in thickness) after cultured in a rotating bioreactor for 4 weeks. The possible reason for this may be that the electrospun fibrous scaffold is a non-woven structure and formed from loosely deposited fibers, which provide little resistance to cell movement. Therefore the cells could push the surrounding fibers aside to expand the pores when they migrate through the pores [22]. Since the porous structure is essential for cell migration, it is important to keep this structure to the most extent. However, during the biomimetic coating, the pore size became smaller inevitably and the fibers seemed to be stiffer. The cell penetration may be hindered by these factors. Such a cell-scaffold interaction needs to be further investigated.

To evaluate the distribution of the mineral content in SBF10_2h, micro-CT scanning was performed. Fig. 4 shows the three-dimensional reconstruction image, in which the PCL fibers are invisible and appear as empty spaces. The picture shows that the calcium phosphate was present through the whole thickness of the scaffold, including the center. It suggests that the biomimetic method is feasible to introduce nucleation and precipitation inside the porous structure. However, the mineral

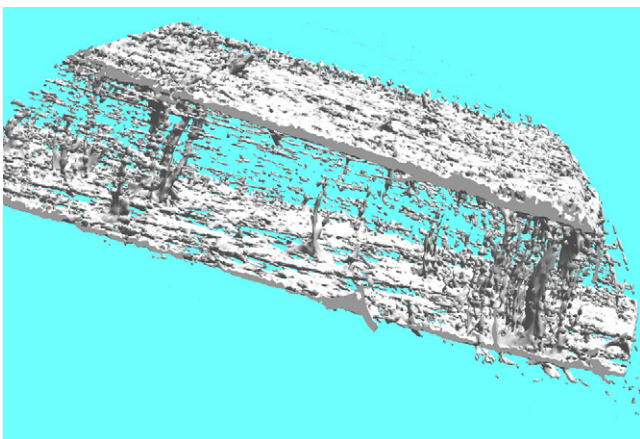


Fig. 4. Microcomputed tomography image of SBF10_2h.

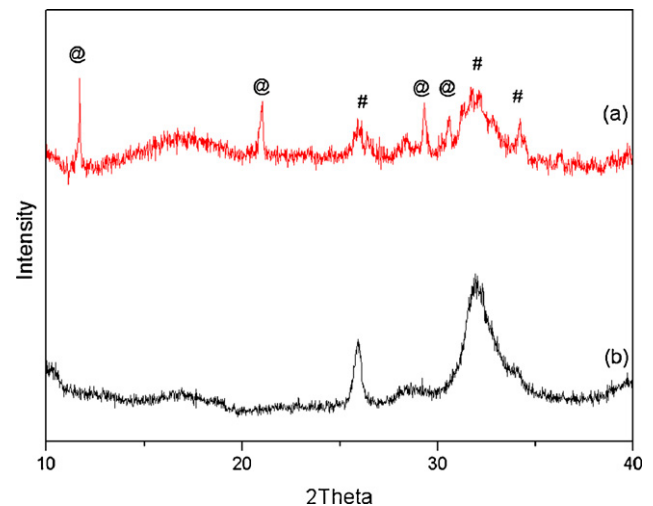


Fig. 5. X-ray diffraction profiles of (a) SBF10_2h and (b) +SBF_7d (@: brushite; #: apatite).

density of the scaffold surface was much higher than that in the center. This may be due to the rate difference of ion diffusion between the surface and center.

To identify the CaP coating on the scaffolds, XRD and FTIR were performed and the results are shown in Figs. 5a and 6a. The XRD data indicated that the coating was a mixture of brushite or dicalcium phosphate dihydrate (DCPD) with apatite. The crystal size of the apatite was estimated to be 30 nm. The FTIR spectrum confirmed the presence of DCPD. An obvious feature of DCPD is the occurrence of two intense doublets in the O–H stretching region: one with components at 3541 and $3488\ \text{cm}^{-1}$ and the other with components at 3286 and $3162\ \text{cm}^{-1}$, which are attributed to the two types of water molecules existing in the unit cell [23]. Another strong peak showing at $1650\ \text{cm}^{-1}$ is attributed to O–H bending. The presence of PO_4 was shown by the bands at 1135 , 1060 (P–O stretching) and 576 , $527\ \text{cm}^{-1}$ (P–O bending). HPO_4 was confirmed by P–OH stretching at $874\ \text{cm}^{-1}$. However, we could not clearly identify the presence of apatite because its peaks overlapped with those of DCPD. The

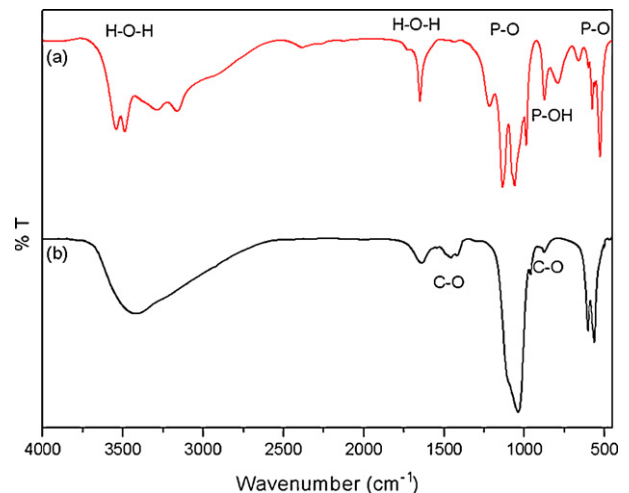


Fig. 6. FTIR spectra of (a) SBF10_2h and (b) +SBF_7d.


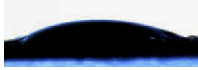
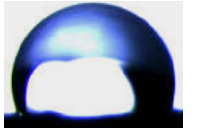
EDS results showed that Ca/P ratio of the coating was around 1–1.2, which is slightly above the Ca/P molar ratio of DCPD (1.0). This may be due to the contribution from apatite whose stoichiometric Ca/P molar ratio is 1.67.

DCPD is speculated to be one of the nucleation precursors of biological apatite from normal and pathological calcifications. Therefore, SBF10_2h was continuously soaked in classical SBF solution for 7 days and the sample was named +SBF_7d. As expected, XRD (Fig. 5b) showed that all DCPD peaks disappeared and only apatite was left in the coating, while the size of the nano-apatite slightly increased from 30 to 43 nm. The FTIR spectrum (Fig. 6(b)) further indicated that the calcium phosphate coating was carbonate apatite. Bands of O-H stretching and bending were seen at 3420 and 1640 cm^{-1} , respectively. The bands at 960 (ν_1), 470 (ν_2), 1040 and 1088 (ν_3), 565 and 602 (ν_4) cm^{-1} were assigned to PO_4 . CO_3^{2-} was recorded at 873, 1420, 1456 and 1544 cm^{-1} , suggesting that the apatite is type B carbonate apatite (CO_3 substituting for PO_4) [24]. The Ca/P ratio of +SBF_7d, as determined by EDS, was about 1.35–1.6, indicating that the coating was calcium deficient. SEM micrographs showed no obvious change in coating morphology after 7 days SBF solution soaking (Fig. 3e). The average fiber diameter slightly increased from 2.2 to 2.3 μm (Table 3). Nevertheless, the weight of +SBF_7d increased enormously, being 21.8% (Table 3). This weight change may be due to the transformation of low-density DCPD to denser apatite and the continuous mineralization of the scaffold.

The process of this surface mineral nucleation and growth is a biomimetic process analogue to several natural processes, including the process of mineral formation in teeth and bones. In general, the structure and composition of the CaP precipitation can be influenced by the ion concentration in the surrounding solution, pH value and temperature. For example, low temperature and pH favors the formation of DCPD and octacalcium phosphate (OCP); higher pH favors the formation of apatite [25]. In our study, the product from SBF10_2h was nano-apatite together with DCPD. DCPD is known to be a nucleation precursor and transforms into the thermodynamically more stable apatitic CaP by a dissolution-reprecipitation mechanism by following the reaction: $10\text{CaHPO}_4 \cdot 2\text{H}_2\text{O} \rightarrow \text{Ca}_{10}(\text{PO}_4)_6(\text{OH})_2 + 4\text{H}_3\text{PO}_4$. DCPD has a relatively low solubility in water; therefore water alone may not be sufficient to drive the reprecipitation mechanism. However, when the aqueous medium of DCPD immersion contains Ca^{2+} ions, the process will readily proceed [26]. Therefore, classical SBF solution was used for the hydrolytic conversion of DCPD, as present in the coating, into apatitic CaP. The slow deposition rate of SBF ensured that the dissolution-reprecipitation mechanism (DCPD into apatite) overwhelmed nucleation-growth mechanism (apatite deposition) in the experimental 7 days.

The results of water wettability and capillary reaction test were shown in Table 4 and Fig. 7, respectively. The results from the water wettability test indicated that the water contact angle of the PCL film decreased from 63° to 24 – 26° after CaP coating, which effect was comparable to that of plasma treatment. The surface of the electrospun PCL scaffold was very hydrophobic,

Table 4
Contact angles of water droplets on different substrates

Sample	Contact angle ($^\circ \pm \text{S.D.}$)	Representative shape of the water drop
PCL film		
Untreated	63 ± 1	
Plasma treated SBF10_2h +SBF_7d	25 ± 2 26 ± 5 24 ± 4	
Electrospun PCL fibers		
Untreated	113 ± 5	
Plasma treated SBF10_2h +SBF_7d	–	Water droplets sinking into the scaffolds

showing a water contact angle of 113° . This increase in contact angle compared to PCL film was due to the surface roughness of the electrospun scaffold [27]. After plasma treatment or CaP coating, the applied water droplets were immediately absorbed by the scaffolds, indicating an improved water wettability of the scaffolds. Similar observations were done in the water capillary reaction test. No capillary action occurs for the electrospun PCL scaffold (Fig. 7a), indicating that the sample was hydrophobic. After plasma treatment, the water front line came up very fast

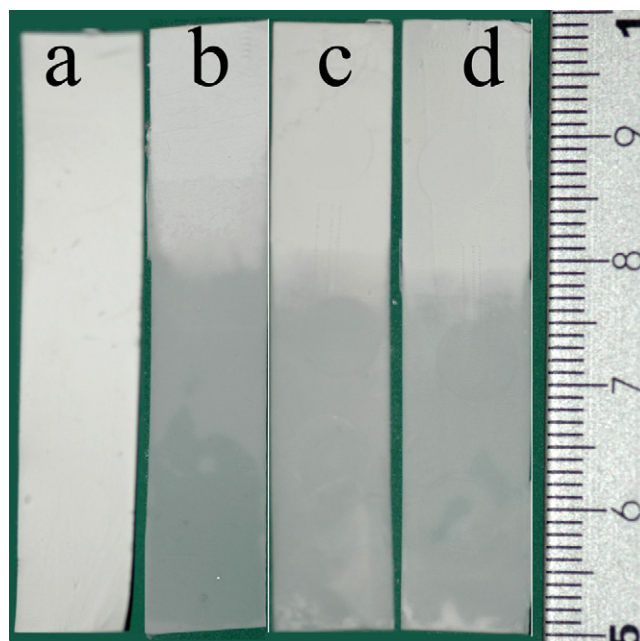


Fig. 7. Water capillary reaction test: no capillary reaction occurred for untreated electrospun PCL scaffold (a); water front reached the height of about 3.0 cm after 30 s for argon plasma treated electrospun PCL scaffold (b); water front reached the height of about 2.7 cm for both SBF10_2h (c) and +SBF_7d (d).

and reached a height of about 3.0 cm after 30 s (Fig. 7b). Comparable capillary reactions for both coated scaffolds, SBF10_2h and + SBF_7d were also observed; the water front lines reached a height of about 2.7 cm (Fig. 7c and d), indicating that the calcium phosphate coating also improved the wettability of the electrospun scaffold. These findings are consistent with previous studies [11,28].

4. Conclusion

The biomimetic method including the plasma surface treatment as reported in this study was efficient to mineralize the electrospun PCL scaffolds with a layer of bone-like apatite. It was shown that the PCL fibers were mineralized after immersion in SBF10 for 2 h (SBF10_2h). After 6 h of incubation, the PCL scaffolds (SBF10_6h) were fully covered with a layer of CaP ceramic and had lost their porous structure. The SBF10_2h coating was found to be composed of a mixture of nano-apatite and dicalcium phosphate dihydrate (DCPD). By continuous immersion in SBF for 7 days, the coating transformed into pure calcium deficient carbonate apatite which is similar to biological apatite. The resulting scaffold has several advantages for bone tissue engineering application. Firstly, the structure mimics natural bone ECM, which is composed of mineralized collagen fibrils. Secondly, the scaffold provides pores for cell migration and nutrient exchange. Thirdly, the coated scaffold is more hydrophilic than the uncoated scaffold. To our knowledge, this study is the first work to successfully coat electrospun PCL scaffold with bioactive CaPs.

Acknowledgements

The authors thank Mr. Vincent Cuijpers and Dr. Frank Walboomers for their assistance on micro-CT and water contact angle analysis. This work was supported by Dutch Program for Tissue Engineering (DPTE) (project number NGT.6730) and the Royal Netherlands Academy of Arts and Sciences (KNAW; project number: 04-PSA-M-02).

References

- [1] A.S. Greenwald, S.D. Boden, V.M. Goldberg, Y. Khan, C.T. Laurencin, R.N. Rosier, Bone-graft substitutes: facts, fictions, and applications, *J. Bone Joint Surg. Am.* 83A (2001) 98–103.
- [2] Y.Z. Zhang, H.W. Ouyang, C.T. Lim, S. Ramakrishna, Z.M. Huang, Electrospinning of gelatin fibers and gelatin/PCL composite fibrous scaffolds, *J. Biomed. Mater. Res. Part B* 72B (2005) 156–165.
- [3] Q.P. Pham, U. Sharma, A.G. Mikos, Electrospinning of polymeric nanofibers for tissue engineering applications: a review, *Tissue Eng.* 12 (2006) 1197–1211.
- [4] R. Murugan, S. Ramakrishna, Nano-featured scaffolds for tissue engineering: a review of spinning methodologies, *Tissue Eng.* 12 (2006) 435–447.
- [5] M. Shin, H. Yoshimoto, J.P. Vacanti, In vivo bone tissue engineering using mesenchymal stem cells on a novel electrospun nanofibrous scaffold, *Tissue Eng.* 10 (2004) 33–41.
- [6] A.S. Badami, M.R. Kreke, M.S. Thompson, J.S. Riffle, A.S. Goldstein, Effect of fiber diameter on spreading, proliferation, and differentiation of osteoblastic cells on electrospun poly(lactic acid) substrates, *Biomaterials* 27 (2006) 596–606.
- [7] R.P. Meinig, B. Rahn, S.M. Perren, S. Gogolewski, Bone regeneration with resorbable polymeric membranes: treatment of diaphyseal bone defects in the rabbit radius with poly(L-lactide) membrane. A pilot study, *J. Orthop. Trauma* 10 (1996) 178–190.
- [8] G.J. Meijer, A. van Dooren, M.L. Gaillard, R. Dalmeijer, C. de Putter, R. Koole, C.A. van Blitterswijk, Polyactive (R) as a bone-filler in a beagle dog model, *Int. J. Oral Maxillofac. Surg.* 25 (1996) 210–216.
- [9] A. Takeuchi, C. Ohtsuki, T. Miyazaki, H. Tanaka, M. Yamazaki, M. Tanihara, Deposition of bone-like apatite on silk fiber in a solution that mimics extracellular fluid, *J. Biomed. Mater. Res. Part A* 65A (2003) 283–289.
- [10] W.L. Murphy, D.H. Kohn, D.J. Mooney, Growth of continuous bone-like mineral within porous poly(lactide-co-glycolide) scaffolds in vitro, *J. Biomed. Mater. Res.* 50 (2000) 50–58.
- [11] Y. Ito, H. Hasuda, M. Kamitakahara, C. Ohtsuki, M. Tanihara, I.K. Kang, O.H. Kwon, A composite of hydroxyapatite with electrospun biodegradable nanofibers as a tissue engineering material, *J. Biosci. Bioeng.* 100 (2005) 43–49.
- [12] J.L. Chen, B. Chu, B.S. Hsiao, Mineralization of hydroxyapatite in electrospun nanofibrous poly(L-lactic acid) scaffolds, *J. Biomed. Mater. Res. Part A* 79A (2006) 307–317.
- [13] F. Yang, C.Y. Xu, M. Kotaki, S. Wang, S. Ramakrishna, Characterization of neural stem cells on electrospun poly(L-lactic acid) nanofibrous scaffold, *J. Biomater. Sci. Polym. Ed.* 15 (2004) 1483–1497.
- [14] T. Kokubo, H. Takadama, How useful is SBF in predicting in vivo bone bioactivity? *Biomaterials* 27 (2006) 2907–2915.
- [15] A.C. Tas, S.B. Bhaduri, Rapid coating of Ti6Al4V at room temperature with a calcium phosphate solution similar to 10× simulated body fluid, *J. Mater. Res.* 19 (2004) 2742–2749.
- [16] Q.P. Pham, U. Sharma, A.G. Mikos, Electrospun poly(epsilon-caprolactone) microfiber and multilayer nanofiber/microfiber scaffolds: Characterization of scaffolds and measurement of cellular infiltration, *Biomacromolecules* 7 (2006) 2796–2805.
- [17] X.F. Walboomers, H.J.E. Croes, L.A. Ginsel, J.A. Jansen, Contact guidance of rat fibroblasts on various implant materials, *J. Biomed. Mater. Res.* 47 (1999) 204–212.
- [18] F. Chen, C.N. Lee, S.H. Teoh, Nanofibrous modification on ultra-thin poly(e-caprolactone) membrane via electrospinning, *Mater. Sci. Eng. C* 27 (2007) 325–332.
- [19] A. Oyane, M. Uchida, C. Choong, J. Triffitt, J. Jones, A. Ito, Simple surface modification of poly(epsilon-caprolactone) for apatite deposition from simulated body fluid, *Biomaterials* 26 (2005) 2407–2413.
- [20] A. Oyane, M. Uchida, Y. Yokoyama, C. Choong, J. Triffitt, A. Ito, Simple surface modification of poly(epsilon-caprolactone) to induce its apatite-forming ability, *J. Biomed. Mater. Res. Part A* 75A (2005) 138–145.
- [21] P. Habibovic, F. Barrere, C.A. van Blitterswijk, K. de Groot, P. Layrolle, Biomimetic hydroxyapatite coating on metal implants, *J. Am. Ceram. Soc.* 85 (2002) 517–522.
- [22] W.J. Li, C.T. Laurencin, E.J. Caterson, R.S. Tuan, F.K. Ko, Electrospun nanofibrous structure: a novel scaffold for tissue engineering, *J. Biomed. Mater. Res.* 60 (2002) 613–621.
- [23] J.W. Xu, I.S. Butler, D.F.R. Gilson, FT-Raman and high-pressure infrared spectroscopic studies of dicalcium phosphate dihydrate (CaHPO₄·2H₂O) and anhydrous dicalcium phosphate (CaHPO₄), *Spectrosc. Acta Pt. A: Mol. Biomol. Spectr.* 55 (1999) 2801–2809.
- [24] R.Z. LeGeros, Calcium Phosphates in Enamel, Dentin and Bone, Calcium Phosphates in Oral Biology and Medicine, Karger, Basel, 1991, pp. 108–129.
- [25] R.Z. LeGeros, Formation and transformation of calcium phosphates: relevance to vascular calcification, *Z. Kardiol.* 90 (2001) III/116–III/124.
- [26] A.C. Tas, S.B. Bhaduri, Chemical processing of CaHPO₄·2H₂O: Its conversion to hydroxyapatite, *J. Am. Ceram. Soc.* 87 (2004) 2195–2200.
- [27] H.M. Shang, Y. Wang, K. Takahashi, G.Z. Cao, D. Li, Y.N. Xia, Nanostructured superhydrophobic surfaces, *J. Mater. Sci.* 40 (2005) 3587–3591.
- [28] K. Fujihara, M. Kotaki, S. Ramakrishna, Guided bone regeneration membrane made of polycaprolactone/calcium carbonate composite nano-fibers, *Biomaterials* 26 (2005) 4139–4147.